

****FULL TITLE****
*ASP Conference Series, Vol. **VOLUME**, **YEAR OF PUBLICATION***
****NAMES OF EDITORS****

X-ray echoes of infrared flaring in Sgr A*

Mark Wardle

*Department of Physics & Engineering, Macquarie University, NSW
 2109, Australia*

Abstract.

Sgr A* exhibits flaring in the infrared several times each day, occasionally accompanied by flaring in X-rays. The infrared flares are believed to arise through synchrotron emission from a transient population of accelerated electrons. The X-ray flaring has been interpreted as self-synchrotron-compton, inverse compton, or synchrotron emission associated with the transient electrons.

Here I consider the upscattering of infrared flare photons by relativistic thermal electrons in the accretion flow around Sgr A*. Typical profiles of electron density and temperature in the accretion flow are adopted and the X-ray light curves produced by upscattering of infrared flare photons by the accretion flow are computed.

Peak X-ray luminosities between 10^{33} and 10^{34} erg s⁻¹ are attained for a 10 mJy near-infrared flare, compatible with observed coincident infrared/X-ray flares from Sgr A*. Even if this process is not responsible for the observed flares it still presents a serious constraint on accretion flow models, which must avoid over-producing X-rays and also predicting observable time lags between flaring in infrared and in X-rays.

Future high-resolution infrared instrumentation will be able to place the location of the infrared flare and in coordination with the X-ray would severely constrain the disc geometry and the radial profiles of electron density and temperature in the accretion flow.

1. Introduction

The quasi-steady emission from Sgr A* spanning radio to submillimeter frequencies is believed to be synchrotron radiation from electrons participating in an accretion flow that extends out to radii of 100 AU or more from the event horizon (e.g. Yuan et al. 2003), or alternatively close the base of a jet (e.g. Falcke & Markoff 2000). The electron temperature and magnetic field strength in the inner regions of the flow are inferred to be $kT_e \sim 10$ MeV and ~ 30 G, respectively.

Several times a day, Sgr A* exhibits dramatic flaring in the near-infrared, with ~ 30 -minute flare durations and peak fluxes (corrected for extinction) ranging downwards from 30 mJy (e.g. Genzel et al. 2003; Eckart et al. 2006b; Yusef-Zadeh et al. 2006, 2009; Do et al. 2009). The emission is highly polarized (Eckart et al. 2006a; Meyer et al. 2006; Trippe et al. 2007) and so the flaring is almost certainly synchrotron emission from a transient population of \sim GeV electrons that are promptly accelerated by a violent event and subsequently cool by synchrotron losses.

A small fraction of infrared flares are accompanied by an X-ray flare which peaks within a few minutes of (and possibly contemporaneously with) the near-infrared (e.g. Baganoff et al. 2001; Porquet et al. 2008). Several scenarios for the X-ray flaring have been considered:

- (i) upscattering of sub-millimeter synchrotron photons by the transient population of GeV electrons that emitted them, ie. self-synchrotron-compton (e.g. Yuan, Quataert & Narayan 2004; Eckart et al. 2004);
- (ii) upscattering of sub-millimeter photons from the accretion flow by the transient GeV electrons (Yusef-Zadeh et al. 2006);
- (iii) upscattering of infrared flare photons by the ~ 10 MeV electrons in the accretion flow (Yusef-Zadeh et al. 2006, 2009); and
- (iv) synchrotron emission from the high energy tail of the accelerated electron population (e.g. Markoff et al. 2001; Yuan, Quataert & Narayan 2003, 2004).

Dodds-Eden et al. (2009) argue that the first three scenarios are unable to produce the observed X-ray fluxes for reasonable parameters. The synchrotron-self-compton scenario requires photons to be produced and subsequently up-scattered all within the same infrared source region. The requisite optical depth to Thomson scattering implies a source region that is unreasonably compact and overpressured relative to its surroundings, with equipartition magnetic field strengths of at least 2 kG. Similarly, in the second scenario, the predicted X-ray flux falls short unless the upscattering rate is boosted by adopting an unreasonably compact millimeter/infrared source region, with an equipartition field strength in excess of 200 G. The third scenario is excluded on the grounds that it should produce a similar X-ray flux as the second. This follows from a fundamental symmetry between scenarios (ii) and (iii): if one chooses any electron from the infrared source region and any from the millimetre-emitting population, then synchrotron photons emitted by one and upscattered by the other will have the same energy; and the cross-section for scattering in both cases is identical (i.e. the Thomson cross section). So then two distinct populations of electrons will produce similar X-ray fluxes by upscattering the synchrotron emission from the other. In addition, Dodds-Eden et al. (2009) note that this scenario implies time-delays between infrared and X-rays and these are strongly constrained by existing data. Instead, they favour synchrotron emission from a high-energy tail of the transient electrons producing the infrared emission.

So are inverse compton scenarios ruled out? No, at least not scenario (iii)! As noted in Yusef-Zadeh et al. (2009), the symmetry argument outlined above implicitly assumes that both electron populations are optically thin to seed and upscattered photons. In contrast, the accretion flow is optically thick to millimeter photons and optically thin to infrared and X-ray photons. Thus many of the millimeter synchrotron photons are reabsorbed and the upscattered flux in (ii) is reduced by a factor of τ relative to scenario (iii). Indeed, Yusef-Zadeh et al. (2009) estimated that the X-ray flux produced by (iii) should be comparable to that observed.

Regardless of the mechanism actually responsible for X-ray flares from Sgr A*, upscattering of infrared flare photons by the accretion flow is efficient enough to constrain the electron density and temperature profiles in accretion models,

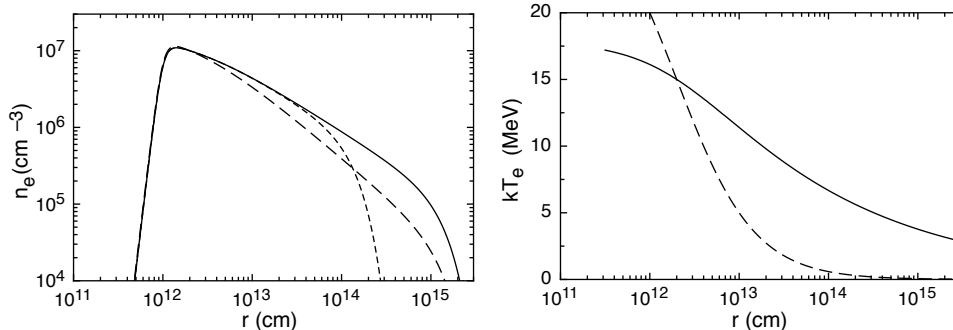


Figure 1. (*Left*) Adopted midplane electron density profiles, with $n_e \propto r^{-0.75}$ (solid and short dashed curves) or r^{-1} with cutoffs at $500 R_s$ and $50 R_s$ (solid or dashed curve respectively). (*Right*) Adopted radial profiles of electron temperature, with $T_e \propto r^{-0.25}$ or $T_e \propto r^{-1}$ (solid or dashed curves respectively).

which must avoid over-producing X-rays and also avoid contradicting the limits on the time lag between flaring in infrared and in X-rays.

To illustrate this, I consider the X-ray emission produced by inverse-compton scattering of infrared flare photons from simple (but reasonable) accretion flow profiles.

2. Calculations

Some justifiable approximations simplify the calculation of the X-ray echo. First, the energy of an upscattered photon with initial energy $h\nu_{\text{infrared}}$ is assumed to be $\gamma^2 h\nu_{\text{infrared}}$ where γ is the electron Lorentz factor; the total production rate of upscattered photons per unit volume is $n_{\text{infrared}} n_e \sigma_{TC}$ where n_{infrared} and n_e are the number densities of infrared photons and relativistic electrons; and the upscattering is assumed to be isotropic. Second, the electron population is characterised by an approximate relativistic maxwellian $f(x) = 1/2x^2 \exp(-x^2)$ where $x = E/kT_e$ (valid for $kT_e \gtrsim 2$ MeV).

The adopted model profiles for the electron density and temperature are $n_e \propto r^{-0.75}$, $T_e \propto r^{-0.25}$ or $n_e \propto r^{-1}$, $T_e \propto r^{-1}$. The density is truncated within $2 R_s$ and beyond $50 R_s$ and is assumed to be either spherically symmetric or disk-like with $h/r = 0.5$. The density and temperature profiles are plotted in Fig. 1. These numbers are within the typical ranges considered in analytic estimates (e.g. Loeb & Waxman 2007, semi-analytic models for the accretion flow (e.g. Yuan, Quataert & Narayan 2003); and MHD simulations (e.g. Mościbrodzka et al. 2009).

For the sake of illustration, we consider an infrared flare with a peak flux of 10 mJy at $2\mu\text{m}$, a gaussian light curve with a 30 minute FWHM, and a $\lambda^{0.5}$ spectrum extending up to $0.2\mu\text{m}$. The infrared emission is assumed to originate from a point source at a specified location. Note that the X-ray echo depends linearly on the flare photons, and an extended flare emission region could easily be modelled as a sum of the responses from a cluster of point sources. Here

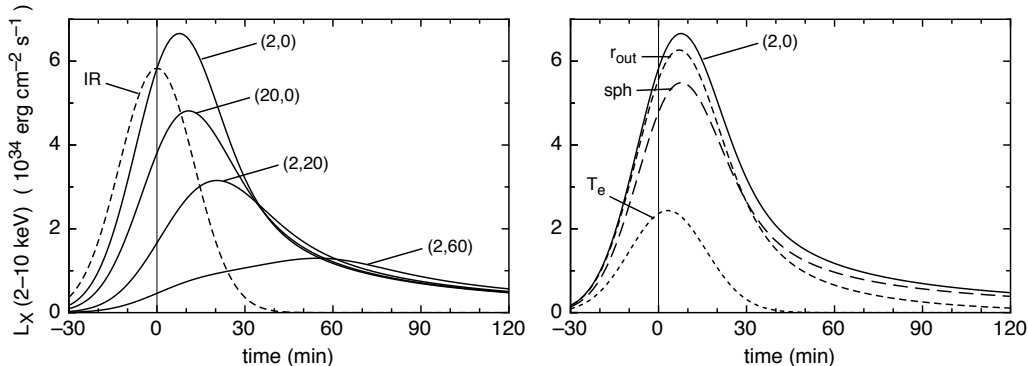


Figure 2. X-ray light curves resulting from inverse Compton scattering of infrared photons produced by a compact infrared flare occurring in the vicinity of Sgr A*. Left panel – solid curves show the resultant X-ray light curves for different locations of the infrared source region, labelled by (r, z) (in units of 10^{12} cm). The dashed curve shows the assumed gaussian profile of the infrared flare which has a 10 mJy peak at $t=0$ and FWHM 30 minutes. Right panel – broken curves show additional light curves for $(r, z) = (2, 0)$ with differing assumptions about the accretion flow: r_{out} reduced from $500R_s$ to $50R_s$ (short dashes); spherically symmetric with the same total number of electrons (long dashes); $T_e \propto r^{-1}$ (dotted).

we focus on this simple model flare and consider a few different positions of the infrared source and explore the effect of changing some of the parameters of the accretion flow.

3. Results

Fig. 2 shows the X-ray response for a variety of infrared flare locations and choices of accretion-flow profiles. First we adopt the density and temperature profile indicated by the solid curves in the left and right panels of Fig. 1 respectively and a disc scale height $h/r = 0.5$. The left panel of Fig. 2 shows the resulting X-ray flare for different choices of infrared source positions. The central concentration of the electron density near the inner edge of the accretion flow and the centrally-concentrated temperature profile means that there is a delay in the peak response of the upscattered X-rays. As the source location is moved successively further away from the inner edge of the disk the delay and width of the profile both increase. The peak flux is correspondingly diminished.

The right hand panel of Fig. 2 shows the effect of varying the adopted accretion flow while keeping the infrared source region at a fixed location. The upscattered X-ray light curve is relatively insensitive to changing the accretion flow outer boundary and aspect ratio (short-dashed and long-dashed curves respectively), but is sensitive to changes to the temperature profile (dotted curve) as the electron temperature controls the fraction of the electrons that are able to upscatter the infrared photons to X-ray energies. In particular, switching from the $T_e \propto r^{-0.25}$ to a steeper $T_e \propto r^{-1}$ profile (solid vs dashed curves in Fig. 1) means that less electrons overall have sufficient energy to upscatter in-

frared photons to X-ray energies, so the peak X-ray flux and total fluence are both reduced. The energetic electrons are concentrated close to the inner edge of the accretion flow, and the reduced physical extent of the relevant electron population reduces the time delay between the infrared and X-ray peaks and eliminates the long tail in the original X-ray light curve.

4. Discussion & Conclusions

The calculations presented above do not include relativistic effects such as lensing, time delays, gravitational redshift, and relativistic beaming of upscattered photons by the bulk motion of the material. All of these effects are important close to the inner edge of the accretion flow and will make a concomitant contribution to the shaping of the lightcurve. In addition, the relative geometry of the infrared flare source location, the black hole and the observers' line of sight are essentially free parameters.

Nevertheless the point remains: upscattering of infrared flare photons by thermal electrons in the accretion flow enveloping Sgr A* will produce significant X-rays. The counterargument by Dodds-Eden et al. (2009, and elsewhere in this volume) that inverse compton scattering is produced only weak X-ray fluxes breaks down because the radio to sub-millimeter emission from the accretion flow is optically thick, so there are more electrons available to upscatter near-infrared photons to X-ray energies than indicated simply based on the millimeter flux from Sgr A*. Typical accretion flow models suggest X-ray flares with peak luminosities of $\sim 10^{33}$ – 10^{34} erg s⁻¹ per mJy of peak flux in the near-infrared, as previously estimated by Yusef-Zadeh et al. (2009).

Independent of whether this process is, or is not, responsible for the observed X-ray flares, models for the accretion flow must not overproduce X-rays, nor predict observable time delays between X-ray and near-infrared flaring in excess of several minutes, nor overproduce extended decay tails. This suggests that the infrared flares occur close to the inner edge of Sgr A* and that the electron temperature with increasing radius falls reasonably rapidly.

Future high-resolution imaging of Sgr A* in the near-infrared with, for example, VLTI/GRAVITY (see the papers by Paumard et al. and Vincent et al. elsewhere in these proceedings) has the potential to strongly constrain the location of the near-infrared flare source. In conjunction with simultaneous monitoring for X-ray flaring this would sharply constrain models for the accretion flow.

Acknowledgments. Thanks to BP Pandey, Charles Gammie, and Farhad Yusef-Zadeh for useful discussions. This work was supported by the Australian Research Council through Discovery Project Grant DP0986386.

References

- Baganoff, F. K., Maeda, Y., Morris, M., Bautz, M. W., Brandt, W. N., Cui, W., Doty, J. P., Feigelson, E. D., Garmire, G. P., Pravdo, S. H., Ricker, G. R. & Townsley, L. K. 2003, *ApJ*, 591, 891
 Do, T., Ghez, A. M., Morris, M. R., Yelda, S., Meyer, L., Lu, J. R., Hornstein, S. D. & Matthews, K. 2009, *ApJ*, 691, 1021

- Dodds-Eden, K., Porquet, D., Trap, G., Quataert, E., Haubois, X., Gillessen, S., Grosso, N., Pantin, E., Falcke, H., Rouan, D., Genzel, R., Hasinger, G., Goldwurm, A., Yusef-Zadeh, F., Clenet, Y., Trippe, S., Lagage, P.-O., Bartko, H., Eisenhauer, F., Ott, T., Paumard, T., Perrin, G., Yuan, F., Fritz, T. K. & Mascetti, L. 2009, *ApJ*, 698, 676
- Eckart, A., Baganoff, F. K., Morris, M., Bautz, M. W., Brandt, W. N., Garmire, G. P., Genzel, R., Ott, T., Ricker, G. R., Straubmeier, C., Viehmann, T., Schödel, R., Bower, G. C. & Goldston, J. E. 2004, *A&A*, 427, 1
- Eckart, A., Schödel, R., Meyer, L., Trippe, S., Ott, T. & Genzel, R. 2006a, *A&A*, 455, 1
- Eckart, A., Baganoff, F. K., Schoedel, R., Morris, M., Genzel, R., Bower, G. C., Marrone, D., Moran, J. M., Viehmann, T., Bautz, M. W., Brandt, W. N., Garmire, G. P., Ott, T., Trippe, S., Ricker, G. R., Straubmeier, C., Roberts, D. A., Yusef-Zadeh, F., Zhao, J. H. & Rao, R. 2006b, *A&A*, 450, 535
- Falcke, H. & Markoff, S. 2000, *A&A* 362, 113
- Genzel, R., Schödel, R., Ott, T., Eckart, A., Alexander, T., Lacombe, F., Rouan, D. & Aschenbach, B. 2003, *Nature*, 425, 934
- Loeb, A. & Waxman, E. 2007, *J. Cosm. Astro-Particle Phys.*, 3, 11
- Markoff, S., Falcke, H., Yuan, F. & Biermann, P. L. 2001, *A&A*, 379, L13
- Meyer, L., Schödel, R., Eckart, A., Karas, V., Dovciak, M. & Duschl, W. J. 2006, *A&A*, 458, L25
- Mościbrodzka, M., Gammie, C. F., Dolence, J. C., Shiokawa, H. & Leung, P. K. 2009, *ApJ*, 706, 497
- Porquet, D., Grosso, N., Predehl, P., Hasinger, G., Yusef-Zadeh, F., Aschenbach, B., Trap, G., Melia, F., Warwick, R. S., Goldwurm, A., Belanger, G., Tanaka, Y., Genzel, R., Dodds-Eden, K., Sakano, M. & Ferrando, P. 2008, *A&A*, 488, 549
- Trippe, S., Paumard, T., Ott, T., Gillessen, S., Eisenhauer, F., Martins, F. & Genzel, R. 2007, *MNRAS*, 375, 764
- Yuan, F., Quataert, E. & Narayan, R. 2003, *ApJ*, 598, 301
- Yuan, F., Quataert, E. & Narayan, R. 2004, *ApJ*, 606, 894
- Yusef-Zadeh, F., Bushouse, H., Dowell, C. D., Wardle, M., Roberts, D., Heinke, C., Bower, G. C., Vila-Vilaró, B., Shapiro, S., Goldwurm, A. & Bélanger, G. 2006, *ApJ*, 644, 198
- Yusef-Zadeh, F., Bushouse, H., Wardle, M., Heinke, C., Roberts, D. A., Dowell, C. D., Brunthaler, A., Reid, M. J., Martin, C. L., Marrone, D. P., Porquet, D., Grosso, N., Dodds-Eden, K., Bower, G. C., Wiesemeyer, H., Miyazaki, A., Pal, S., Gillessen, S., Goldwurm, A., Trap, G. & Maness, H. 2009, *ApJ*, 706, 348